

## 1.7 Orbits in axisymmetric potentials

We have seen above that empirically, most galaxies are *not* spherically symmetric, but rather have flattened disks or ellipsoidal shapes. For many of these more general potentials, azimuthal symmetry and also up-down symmetry ( $z \rightarrow -z$ ) are still fine approximations. Thus we can write the potential as  $\Phi(R, \phi, z) = \Phi(R, |z|)$ . From the formula for the gradient in cylindrical coordinates, we get the three pieces of the vector equation  $\ddot{\mathbf{r}} = -\vec{\nabla}\Phi$ ,

$$\begin{aligned}\hat{\mathbf{e}}_R &: \ddot{R} - R\dot{\phi}^2 = -\frac{\partial\Phi}{\partial R} \\ \hat{\mathbf{e}}_\phi &: \frac{d}{dt}(R^2\dot{\phi}) = 0 \\ \hat{\mathbf{e}}_z &: \ddot{z} = -\frac{\partial\Phi}{\partial z}.\end{aligned}\tag{1.89}$$

Just as in the spherically symmetric case, we can define an effective potential  $\Phi_{\text{eff}}$  for a given angular momentum about the  $z$ -axis,  $L_z = R\dot{\phi}^2$ ,

$$\Phi_{\text{eff}} = \Phi + \frac{L_z^2}{2R^2} .\tag{1.90}$$

The equation of motion in the  $\hat{\mathbf{e}}_R$  direction is

$$\ddot{R} = -\frac{\partial\Phi_{\text{eff}}}{\partial R} ,\tag{1.91}$$

(Continued on next page.)

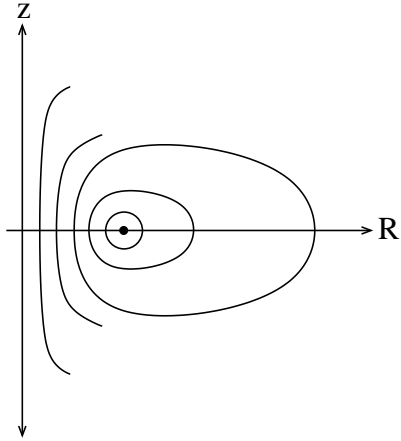


Figure 1.15: Contours of constant of constant  $\Phi_{\text{eff}}$  which are also bounding curves for orbits with energy  $E$ . The dot indicates the “parent” circular orbit, for which  $\Phi_{\text{eff}}$  is a minimum. As  $E$  increases the bounding curves grow larger.

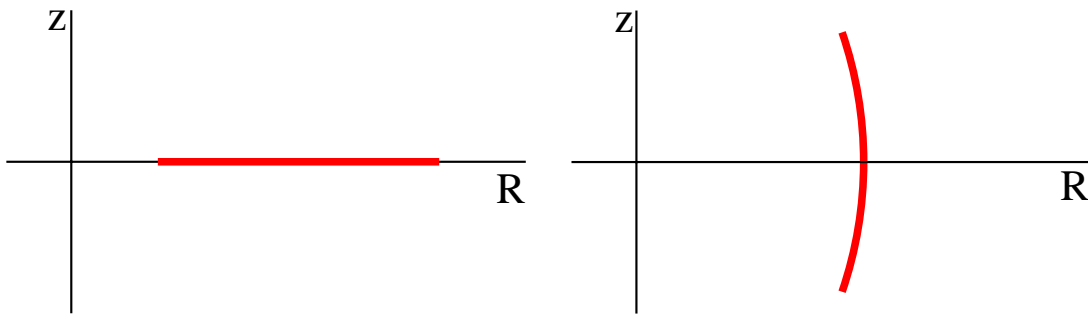


Figure 1.16: Left: A circular orbit has been perturbed in the  $R$  direction. Right: A circular orbit has been perturbed in the  $z$  direction.

the equation of motion in the  $z$  direction is

$$\ddot{z} = -\frac{\partial \Phi_{\text{eff}}}{\partial z} \quad , \quad (1.92)$$

and the energy equation is

$$E = \frac{1}{2}(\dot{R}^2 + \dot{z}^2) + \Phi_{\text{eff}}. \quad (1.93)$$

If we draw curves of constant effective potential (Fig. 1.15), we see that for a given  $L_z$  the minimum effective energy is at a point  $R_g$  on the  $R$  axis. A particle with exactly this minimum energy will be in circular orbit, with orbital frequency  $\Omega$  such that

$$\Omega^2 = \frac{1}{R} \frac{\partial \Phi}{\partial R} \quad . \quad (1.94)$$

We can expand the effective potential in the vicinity of this point,

$$\Phi_{\text{eff}} \approx \Phi(R_g, 0) + \frac{1}{2} \left( \frac{\partial^2 \Phi_{\text{eff}}}{\partial R^2} \right)_{(R_g, 0)} x^2 + \frac{1}{2} \left( \frac{\partial^2 \Phi_{\text{eff}}}{\partial z^2} \right)_{(R_g, 0)} z^2 \quad , \quad (1.95)$$

where we have defined a radial displacement,  $x \equiv R - R_g \ll R_g$ .

If a test particle in circular orbit is given a small perturbation in the radial direction, (Fig. 1.16), it obeys the equation of motion

$$\ddot{x} + \kappa^2 x = 0 \quad \text{where} \quad (1.96)$$

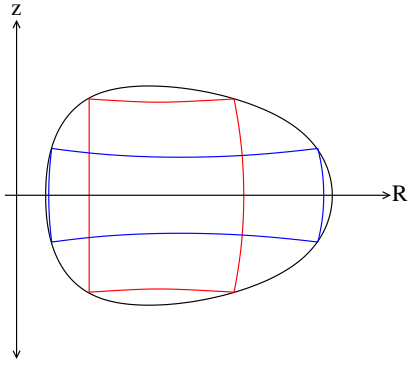


Figure 1.17: Bounding curves for two orbits with the same values of  $E$  and  $L_z$ . Evidently there is some third conserved quantity that makes for distinct bounding curves.

$$\kappa^2 \equiv \left( \frac{\partial^2 \Phi_{\text{eff}}}{\partial R^2} \right)_{(R_g, 0)} \quad (1.97)$$

defines the *epicyclic frequency*,  $\kappa$ .

Similarly giving a particle given a small perturbation perpendicular to the orbital plane (Fig. 1.16) will obey the equation of motion

$$\ddot{z} + \nu^2 z = 0 \quad \text{where,} \quad (1.98)$$

$$\nu^2 \equiv \left( \frac{\partial^2 \Phi_{\text{eff}}}{\partial z^2} \right)_{(R_g, 0)} \quad (1.99)$$

defines the vertical frequency  $\nu$ .

As the amplitudes of the the perturbations increase the expansion above is no longer strictly correct, but the character of the two orbits remains the same. In one case the particle oscillates within the orbital plane, while in the other the particle traces out an arc in the  $(R, z)$ , *meridional plane*. Notice that the epicyclic, vertical and orbital frequencies need not be the same – in general they *are* different. Only for the Kepler potential and for the spherical harmonic potential are they identical.

More generally, a particle given an arbitrary perturbation must be contained within the contour  $\Phi_{\text{eff}} = E$  in Figure 1.15. But when a circular orbit is given an arbitrary perturbation, the orbit does not fill the allowed region. Rather it produces a Lissajou figure contained within a box-shaped region. (Fig. 1.17). Notice that two different box-shaped regions can have the same bounding energy. This suggests that some additional conserved quantity, another integral of the motion (beyond energy and  $z$ -axis angular momentum), denies it access to the full allowed region.

To study the dimensionality of these orbits, one constructs a Poincare *surface of section* which reduces the six-dimensional phase space to something more manageable. The construction proceeds as follows:

- a) From azimuthal symmetry, ignore  $\phi$  and  $\dot{\phi}$ , giving 4-D trajectories in  $(R, \dot{R}, z, \dot{z})$ .
- b) Use conservation of energy to give  $\dot{z} = \dot{z}(R, \dot{R}, z, E)$
- c) Take a cross-section of the orbits, plotting a point on the  $(R, \dot{R})$  plane every time the orbit crosses the plane defined by  $z = 0$  with  $\dot{z} > 0$ .

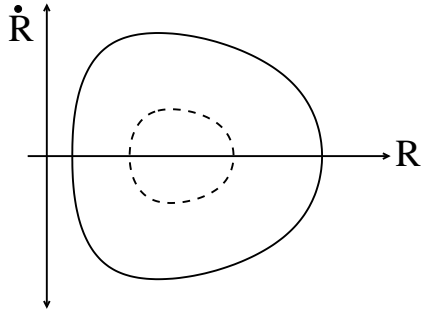


Figure 1.18: A “surface of section”. The allowed region is bounded by the solid curve. The dashes indicate where the particle intersects the  $z = 0$  plane.

- d) The confinement of trajectories to 1-D invariant curves in the  $(R, \dot{R})$  plane suggests they will occupy 2-D surfaces in  $(R, \dot{R}, z, \dot{z})$  space and 3-D regions within the full 6-D phase space and thus the existence of an additional integral of the motion.

An example of such a Poincare surface of section is shown in Figure 1.18.

For potentials that are nearly spherical, the third integral is something like, but not exactly, the total angular momentum. For orbits that stay close to the equatorial plane, the third integral is something like, but not exactly, the energy in the  $z$  direction. More generally, while one may demonstrate the existence of a third integral using Poincare’s method, it cannot be written in closed form<sup>5</sup>.

### 1.7.1 nearly circular orbits: the epicyclic approximation

For many axisymmetric potentials, we are interested primarily in trajectories that are nearly circular with an average orbital frequency  $\Omega(R)$  at each radius  $R$ . This circular orbit acts as a *guiding center* for the perturbed orbit which we want to study. Near this equilibrium orbit, we can expand the effective potential around the guiding radius  $R_g$  and the equatorial plane  $z = 0$ ,

$$\Phi_{\text{eff}} \approx \Phi(R_g, 0) + \frac{1}{2} \left( \frac{\partial^2 \Phi_{\text{eff}}}{\partial R^2} \right)_{(R_g, 0)} x^2 + \frac{1}{2} \left( \frac{\partial^2 \Phi_{\text{eff}}}{\partial z^2} \right)_{(R_g, 0)} z^2 \quad . \quad (1.100)$$

We pay attention here only to motion in the plane, which decouples from the vertical motion, and henceforth take  $z$  to be identically zero. As before we take the  $x$  direction to be radial and the  $y$  direction to be positive in the direction of rotation. As noted in the previous section, small oscillations are governed by the harmonic equation

$$\ddot{x} + \kappa^2 x = 0 \quad (1.101)$$

and  $\kappa^2$ , defined by equation (1.97), is then

$$\kappa^2 = \left( \frac{\partial^2 \Phi}{\partial R^2} \right)_{R_g} + \frac{3L_z^2}{R_g^4} = \left( R \frac{d}{dR} \Omega^2 + 4\Omega^2 \right)_{R_g} \quad . \quad (1.102)$$

<sup>5</sup>An interesting counterexample is the tri-axial Stäckel potential where all three integrals of motion *can* be written in closed form.

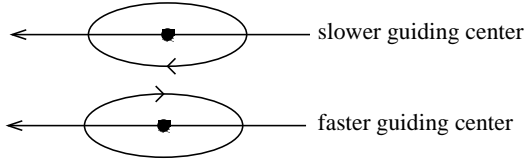


Figure 1.19: Stars executing epicycles around guiding centers or circular orbits. The inner orbit has a higher orbital frequency.

Recall from equation (1.15) the relation between circular velocity and potential gives the orbital frequency as

$$\Omega^2 = \frac{1}{R} \frac{\partial \Phi}{\partial R} = \frac{L_z^2}{R^4}. \quad (1.103)$$

The solutions to (1.101) are harmonic oscillations of the form

$$x(t) = X \cos(\kappa t + \psi), \quad (1.104)$$

where  $\psi$  is a phase determined by initial conditions.

But what is happening in the  $\phi$  direction as the particle executes radial oscillations? The angular position in the orbit can be solved for using conservation of angular momentum and the fact that that  $x \ll R_g$ ,

$$\dot{\phi} = \frac{L_z}{R^2} = \frac{L_z}{R^2 \left(1 + \frac{x}{R_g}\right)^2} \approx \Omega_g \left(1 - \frac{2x}{R_g}\right). \quad (1.105)$$

From here we integrate to get

$$\phi(t) = \Omega_g t + \phi_o - \frac{2\Omega_g}{\kappa R_g} X \sin(\kappa t + \psi). \quad (1.106)$$

It is useful to define  $y$  as the distance away from the guiding circular orbit in the angular direction:

$$y \equiv R_g(\phi - \phi_g) = -\frac{2\Omega_g}{\kappa} X \sin(\kappa t + \psi) = Y \sin(\kappa t + \psi). \quad (1.107)$$

As both the  $x$  and  $y$  coordinates execute harmonic oscillations with the same frequency,  $\kappa$ , the trajectories trace out ellipses, called *epicycles* around the guiding center<sup>6</sup>. A few helpful relations can be derived without too much effort:

$$\frac{1}{2} < \frac{X}{Y} = \frac{\kappa}{2\Omega_g} < 1, \quad (1.108)$$

where the lower bound (1/2) corresponds to a Keplerian potential and the upper bound (1) corresponds to a harmonic potential. Averaging over an epicycle ( $\kappa t = 0 \rightarrow 2\pi$ ), we find

$$\frac{\langle \dot{y}^2 \rangle_{\text{orbit}}}{\langle \dot{x}^2 \rangle_{\text{orbit}}} = \frac{4\Omega_g^2}{\kappa^2}. \quad (1.109)$$

<sup>6</sup>Ptolemy is unjustly ridiculed for having introduced epicycles to explain planetary motions 2000 years ago. Epicycles do indeed improve upon circular motion. What Ptolemy failed to realize was that for planetary motion these epicycles are ellipses rather than circles.

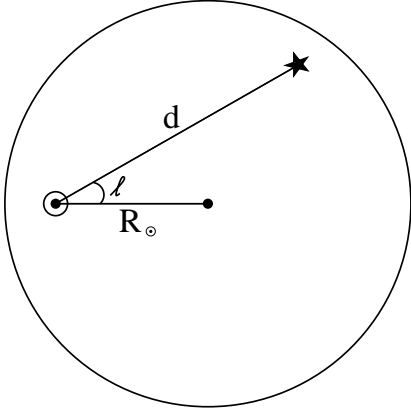


Figure 1.20: A star at distance  $d$  from the sun observed in the plane of the Milky Way at galactic longitude  $l$ . The sun is located a distance  $R_{\odot}$  from the origin at the center of the galaxy.

However, if one takes the average over a volume of space encompassing many orbits instead of just averaging over a single orbit (something we postpone discussing until our treatment of Jeans' equations), one finds the exact opposite:

$$\frac{\langle \dot{y}^2 \rangle_{\text{vol}}}{\langle \dot{x}^2 \rangle_{\text{vol}}} = \frac{\kappa^2}{4\Omega_g^2}. \quad (1.110)$$

A qualitative understanding for this can be seen in Figure 1.19, where the outer, slower guiding center overlaps with a faster inner guiding center but their epicyclic velocities are in opposite directions.

In the early part of this century, Jan Oort interpreted nearby stellar radial velocity and transverse proper motion measurements as the result of differential rotation, giving  $\Omega$  as a function of  $R$ . From the point of view of an observer moving on a circular orbit at distance  $R$  from the center of the galaxy, a star at a distance  $d$  and galactic longitude  $l$  (see Figure 1.20) will have a line-of-sight radial velocity given by

$$v_{\text{los}} = d(A \sin 2l) \quad (1.111)$$

and a transverse velocity of

$$v_T = d(A \cos 2l + B), \quad (1.112)$$

which is actually measured in terms of a proper motion (typically fractions of an arcsecond per yr),

$$\mu = v_T/d = A \cos 2l + B. \quad (1.113)$$

Here  $A$  and  $B$  are the *Oort constants* defined as

$$A \equiv -\frac{1}{2}R \frac{d\Omega}{dR} \quad (1.114)$$

and

$$B \equiv -\left(\frac{1}{2}R \frac{d\Omega}{dR} + \Omega\right). \quad (1.115)$$

From our definitions of the epicyclic frequency, equation (1.97) and Oort's constants we derive

$$\kappa^2 = -4B(A - B). \quad (1.116)$$

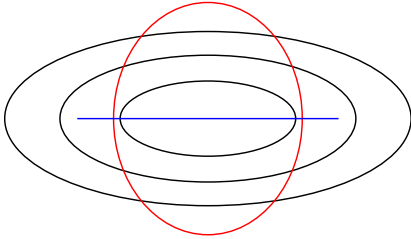


Figure 1.21: The black ellipses are equipotentials. The blue horizontal line is the radial orbit that is the parent of the box orbits. The red ellipse is the closed orbit that is the parent of the tube orbits.